

**Total internal reflection-based single-vesicle in situ quantitative
and stoichiometric analysis of tumor-derived exosomal
microRNAs for diagnosis and treatment monitoring**

Dinggeng He^{1,2}, Huizhen Wang², See-Lok Ho¹, Hei-Nga Chan¹, Luo Hai², Xiaoxiao He²,
Kemin Wang², Hung-Wing Li^{1,2}

1. Department of Chemistry, Hong Kong Baptist University, Kowloon Tong, Hong Kong, China.
2. State Key Laboratory of Chemo/Biosensing and Chemometrics, College of Chemistry and Chemical Engineering, College of Biology, Hunan University, Changsha, China.

Corresponding author: Hung-Wing Li, email: hwli@hkbu.edu.hk

Supporting Information

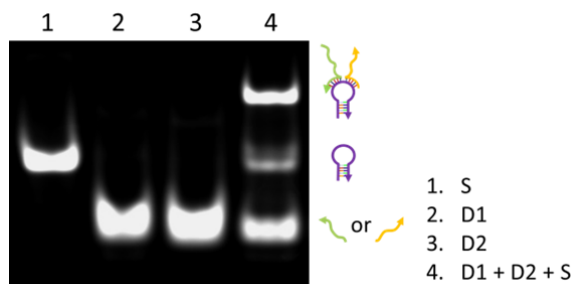


Figure S1. Gel electrophoresis image showing the self-assembly of the SDP (lane 4). S represents the DNAzyme substrate, but without fluorescent dye and quencher.

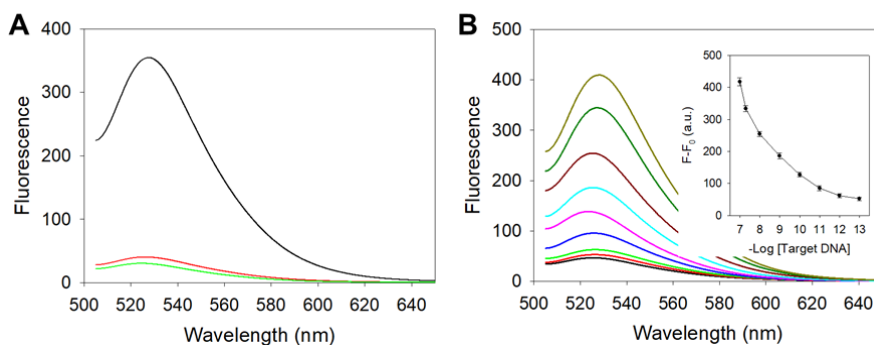


Figure S2. Fluorescence tests of SDP21 in buffer. **(A)** Fluorescence changes under different conditions: D1, D2, S, Mg^{2+} and miR-21 (black); D1, D2, S, Mg^{2+} and random DNA (red); D1, D2, S and Mg^{2+} (green). **(B)** Fluorescence spectra of the detection system in the presence of target miR-21 with different concentrations (from bottom to top: 0 pM, 0.1 pM, 1 pM, 10 pM, 100 pM, 1 nM, 10 nM, 50 nM and 100 nM). Inset: The relationship between the fluorescence intensity (at 526 nm) and the target concentration at logarithmic scale.

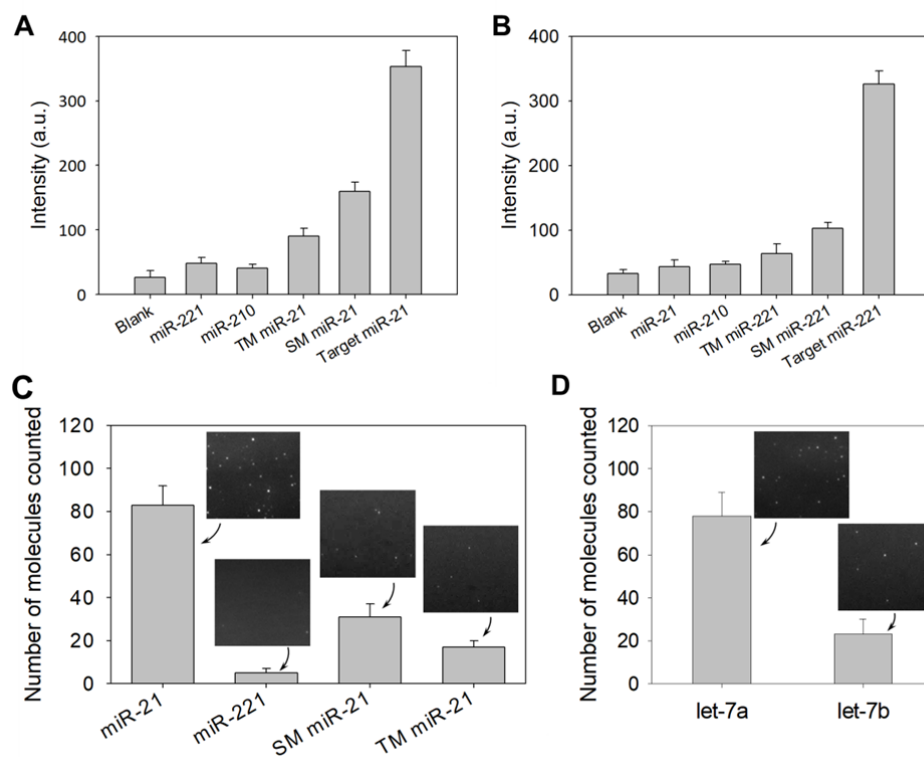


Figure S3. Specificity investigations. Fluorescence changes of SDP21 (**A**) and SDP221 (**B**) in the presence of various sequences. The reaction time was 40 min. The concentration used for all detected sequence was 50 nM. Number of observed fluorescent spots in TIRF images of various sequences after treatment with MB21 (**C**) and MB7a (**D**), respectively. The concentration used for all detected sequence was 50 pM and the probes concentration was 200 pM. Inset: TIRF images under different conditions. The data depict the averages of three experiments, and the error bars are the standard error of mean of the three trials.

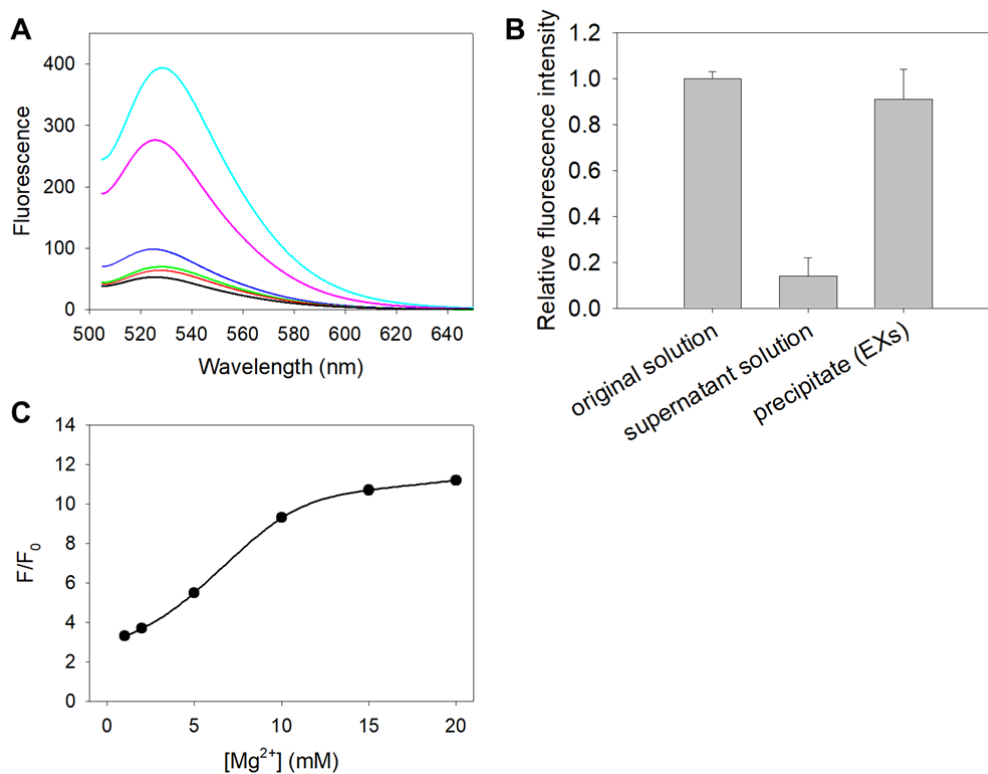


Figure S4. Fluorescence tests of SDP21 after penetration into A375 EXs. **(A)** Fluorescence changes under different conditions: D1, D2, S, Mg²⁺, SLO and A375 EXs (cyan); D1, D2, S, Mg²⁺ and A375 EXs (pink); D1, D2, S, Mg²⁺, SLO and NHEM-c EXs (blue); D1, D2, S, SLO and A375 EXs (green); S, Mg²⁺, SLO and A375 EXs (red); D1, D2, S, Mg²⁺ and SLO (black). **(B)** Investigation of exosomal miR-21 release during SLO treatment by ultracentrifugation (110,000 g, 4 h). The supernatant solutions after ultracentrifugation show a weak fluorescence, while the precipitates (EXs) have a strong fluorescence comparable to the original solution. All values are mean \pm SD (n = 3). **(C)** Optimization of Mg²⁺ concentration.

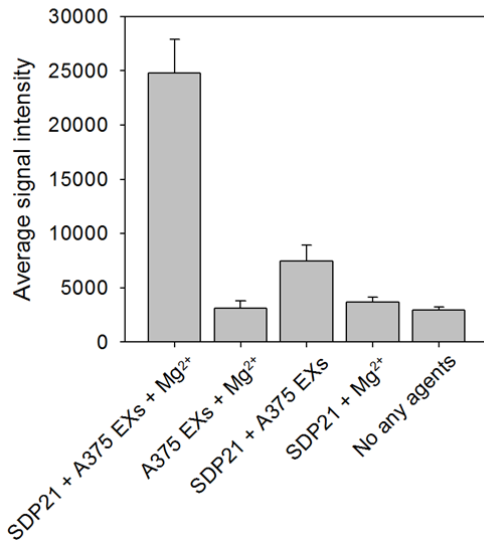


Figure S5. Average fluorescence intensities of A375 EXs in negative controls (SDP21 + A375 EXs, A375 EXs + Mg²⁺, and SDP21 + Mg²⁺) versus positive sample (SDP21 + A375 EXs + Mg²⁺).

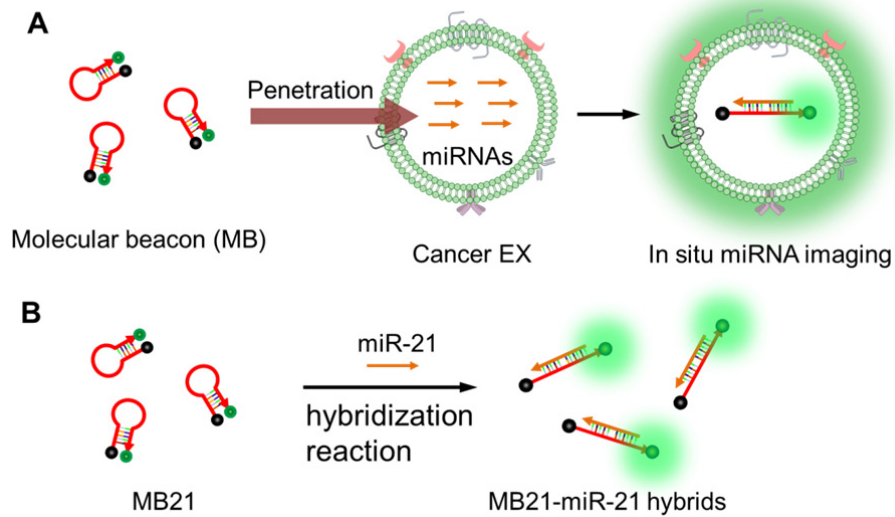


Figure S6. (A) Schematic illustration of the in situ imaging of exosomal miRNAs using MB. **(B)** Schematic illustration of the MB21-miR-21 hybrids formed in EX-free serum.

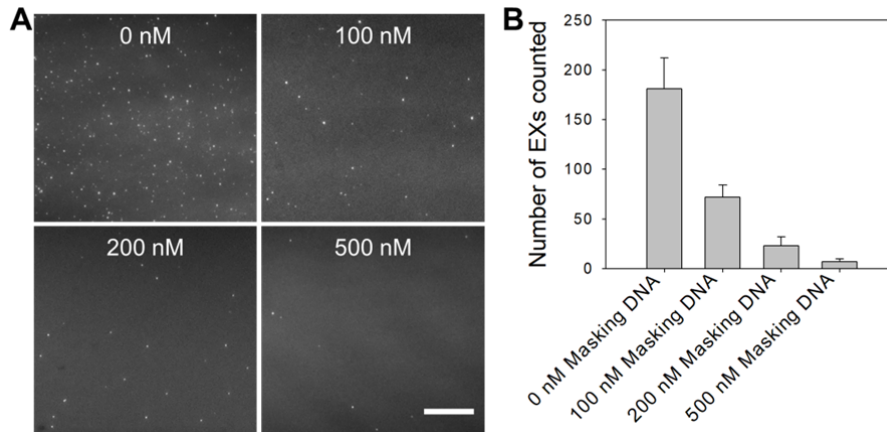


Figure S7. Investigation of hybridization of exosomal miR-21 and MB21 using masking DNA. TIRF images **(A)** and the counted number of fluorescent EXs **(B)** after being pretreated with different concentrations of masking DNA. Scale bar = 3 μ m.

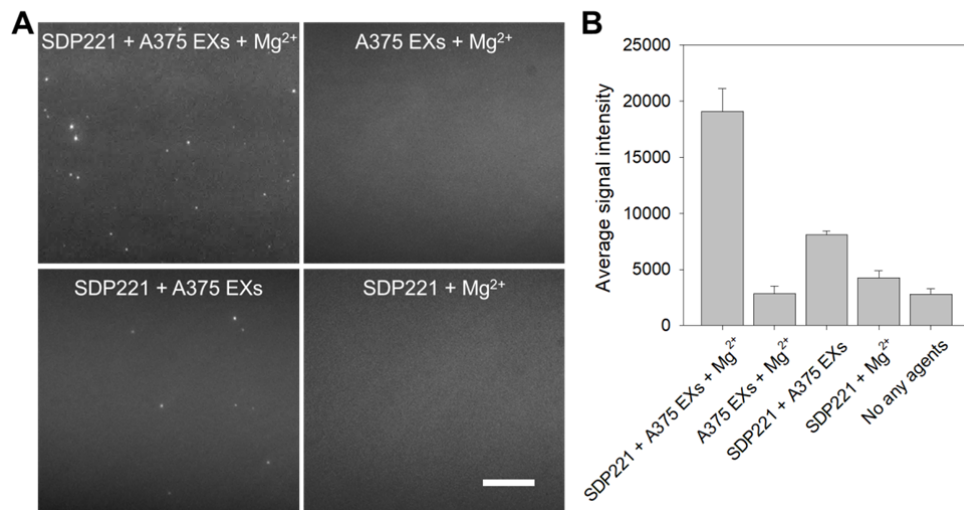


Figure S8. Characterization of the performance of the TIRF assay for exosomal miR-221. TIRF images **(A)** and average signal intensities of A375 EXs **(B)** under different conditions: SDP221 + A375 EXs + Mg²⁺, A375 EXs + Mg²⁺, SDP221 + A375 EXs, and SDP221 + Mg²⁺. Scale bar = 3 μ m.

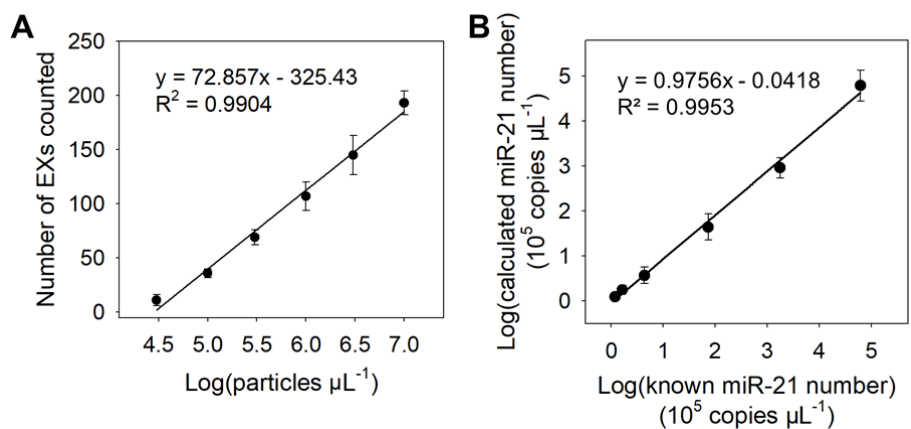


Figure S9. Sensitivity investigations. **(A)** Number of miR-21-EXs with log(EX concentration in EX-spiked serum samples). **(B)** Linear range of the log(TIRF-calculated miR-21 copy numbers) vs log(miR-21 copy numbers determined by qRT-PCR) in EX-spiked standard samples.

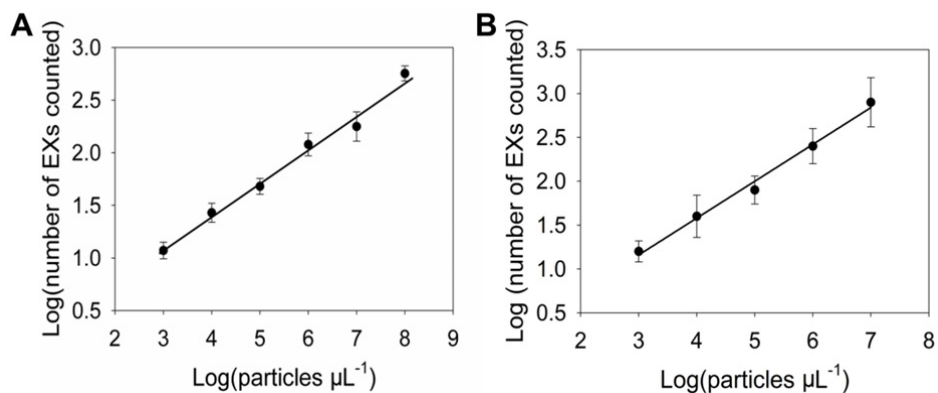


Figure S10. The TIRF assays for total EXs quantification. **(A)** Correlation of log counts of EX-CD63_{apt} nanocomposites with log(EXs concentration in EX-spiked serum samples). **(B)** Correlation of log counts of EX-DiO hybrids with log(EXs concentration in EX-spiked serum samples).

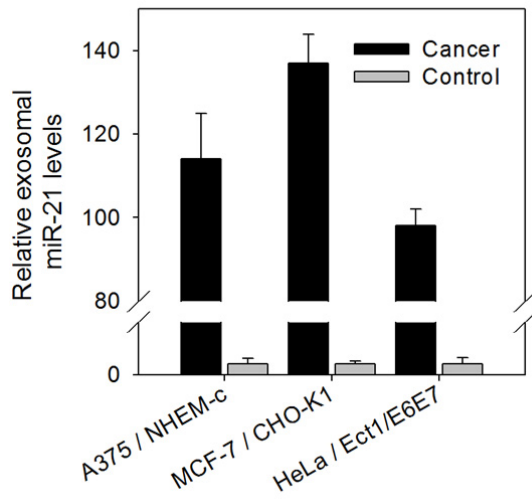


Figure S11. Real-time PCR analysis for exosomal miR-21. EXs were produced from cancer cells (A375, MCF-7 and HeLa cells) and their control cells (NHEM-c, CHO-K1 and Ect1/E6E7 cells), and then isolated by using ExoQuick-TC. The same amount of RNAs from each EX was used for real-time PCR analysis for comparison. The miRNA levels in cancer EXs were normalized by that in their control EXs, respectively.

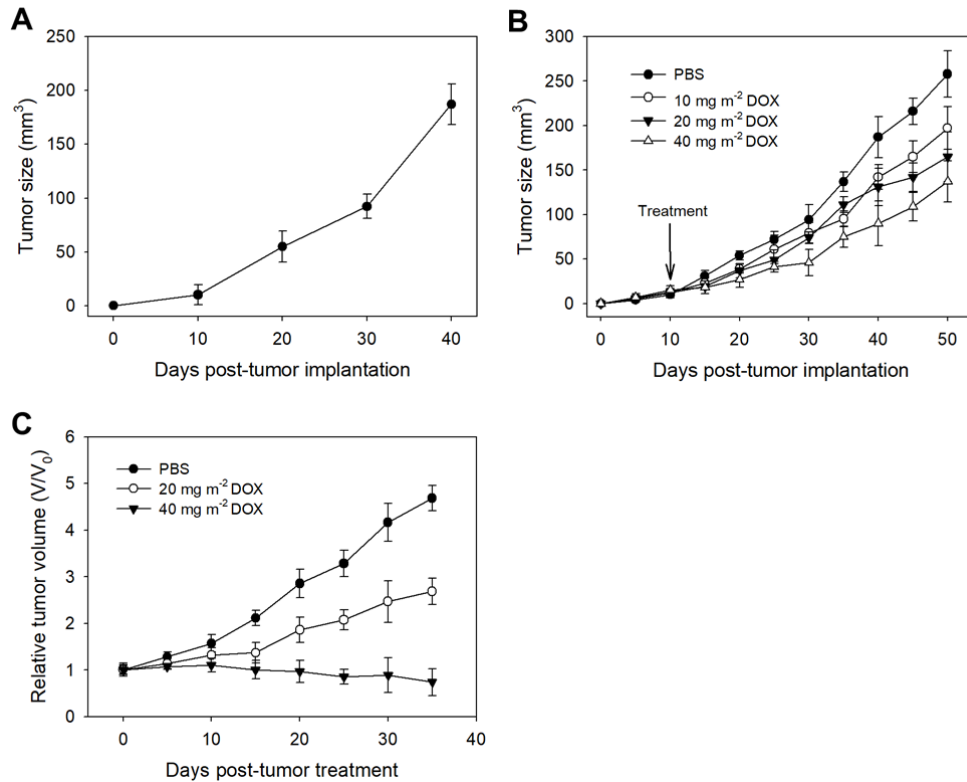


Figure S12. Tumor growth of mice. **(A)** Correlation of tumor size with time post-injection in nude mice subcutaneously injected with A375 cells (2×10^6). **(B)** Changes of tumor sizes after subcutaneous injection with A375 cells for different times. Tumor-bearing mice were treated with different dosages of DOX, respectively, at 10 days post-injection. **(C)** Changes of relative tumor volume (V/V_0) upon different treatments. Tumor volumes (V) were normalized to their initial values (V_0). The treatment of tumor-bearing mice started at 25 days post-injection. The different dosages (20 and 40 mg m^{-2}) of DOX were injected into the abdominal cavity of mice once every 10 days.

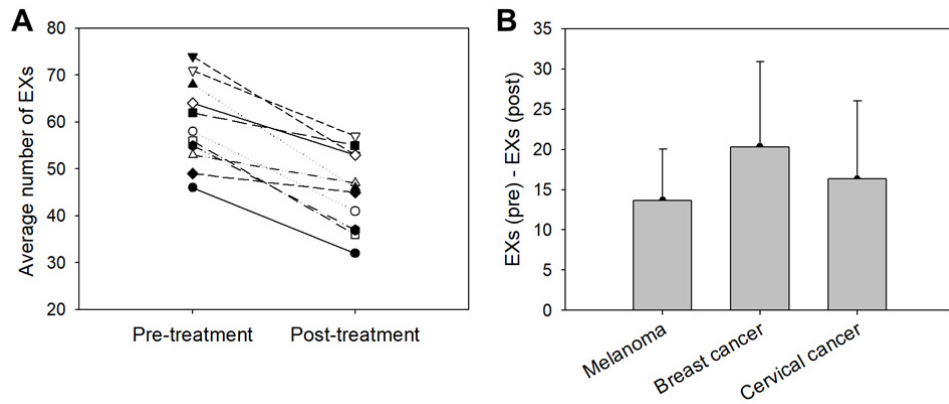


Figure S13. Treatment monitoring based on the single-vesicle imaging analysis of exosomal miR-21. **(A)** The miR-21-EXs levels in the serum samples of tumor-bearing mice ($n = 11$) before and after treatment with DOX (40 mg m^{-2} per 10 days) for 40 days. **(B)** The relative pre-to-post therapy differences of different cancer patients. Changes in miR-21-EXs levels are associated with treatment response.

Table S1. DNA sequences used in this work.

Name	Sequences (5'-3')
miR-21	UAG CUU AUC AGA CUG AUG UUG A
SM miR-21	UAG CUU AUA AGA CUG AUG UUG A
TM miR-21	UAG CUU AUA AGC CUG CUG UUG A
miR-221	GCU ACA UUG UCU GCU GGG UUU C
SM miR-221	GCU ACA UUG UCU GCU GAG UUU C
TM miR-221	GCU AAA UCG UCU GCU GAG UUU C
miR-210	CUG UGC GUG UGA CAG CGG CUG A
D1	CCT CTC GAT ATC AGC GAT CTT CTG ATA AGC TA
D2	TCA ACA TCA GTA AGC ACC CAT GTT ACT CTC CC
D3	CCT CTC GAT ATC AGC GAT CTA GAC AAT GTA GC
D4	GAA ACC CAG CTA AGC ACC CAT GTT ACT CTC CC
S	BHQ1- GCA GCA GAA AAA AAA AAA GGG AGA GTA TrAG GAT ATC GAG AGG AAA AAA AAA ATC TGC TGC -FAM
Fluorescent DNA	GCA GCA GAA AAA AAA AAA GGG AGA GTA TAG GAT ATC GAG AGG AAA AAA AAA ATC TGC TGC -FAM
MB21	BHQ1-GCG CGT CAA CAT CAG TCT GAT AAG CTA CGC GC -FAM
Control MB	BHQ1-GCG CGT CTC TGC CTA AGT GAT GTC ACG CGC -FAM
CD63 aptamer	FAM- CAC CCC ACC TCG CTC CCG TGA CAC TAA TGC TA
Let-7a	UGA GGU AGU AGG UUG UAU AGU U
Let-7b	UGA GGU AGU AGG UUG UGU GGU U
MB7a	BHQ1-GCG CGA ACT ATA CAA CCT ACT ACC TCA CGC GC -FAM
Masking DNA for miR-21	TCA ACA TCA GTC TGA TAA GCT A

SM: single-base mismatched RNA; TM: three-base mismatched RNA. D1 and D2: split DNAzyme for sensing miR-21; D3 and D4: split DNAzyme for sensing miR-221; S: DNAzyme substrate; MB21: molecular beacon for sensing miR-21; MB7a: molecular beacon for sensing let-7a.

Table S2. Average copy numbers of miRNAs determined by qRT-PCR analysis.

Samples	Total EXs (particles μL^{-1})	miRNAs (copies μL^{-1})	
		miR-21	miR-221
A375	2.32×10^9	7.91×10^7	1.58×10^7
NHEM-c	4.15×10^8	2.03×10^5	9.37×10^4

Table S3. Estimated EX concentrations in different cell culture supernatants.

Samples	Total EXs ^a (particles μL^{-1})	Total EXs ^b (particles μL^{-1})	Total EXs ^c (particles μL^{-1})	miR-21-EXs ^d (particles μL^{-1})	miR-221-EXs ^e (particles μL^{-1})
A375	2.32×10^9	8.53×10^8	9.37×10^8	1.53×10^7	5.37×10^6
NHEM-c	4.15×10^8	2.69×10^8	3.39×10^8	7.25×10^3	4.71×10^4

^aNanoSight-generated EXs concentration.

^bCalculated by TIRF assay with the fluorescently-labelled CD63_{apt}.

^cCalculated by TIRF assay with the DiO that is a green fluorescent dye for staining cell membrane.

^dCalculated by TIRF assay with the SDP21.

^eCalculated by TIRF assay with the SDP221.